A comparison of FBG- and Brillouin-strain sensing in the framework of a decameter-scale hydraulic stimulation experiment

Conference Paper · May 2018

CITATIONS
6

READS
760

6 authors, including:

Hannes Krietsch
RWTH Aachen University
57 PUBLICATIONS **641** CITATIONS
SEE PROFILE

Valentin Gischig
ETH Zurich
119 PUBLICATIONS **2,171** CITATIONS
SEE PROFILE

Mohammadreza Jalali
RWTH Aachen University
115 PUBLICATIONS **776** CITATIONS
SEE PROFILE

Joseph Doetsch
ETH Zurich
144 PUBLICATIONS **2,447** CITATIONS
SEE PROFILE

ARMA 18–0800

A comparison of FBG- and Brillouin-strain sensing in the framework of a decameter-scale hydraulic stimulation experiment

Krietsch, H., Gischig, V., Jalali, M.R., Doetsch, J.
Department of Earth Sciences, ETH Zurich, Switzerland
Valley, B.
Center for Hydrogeology and Geothermics, University of Neuchâtel, Switzerland
Amann, F.
Chair of Engineering Geology, RWTH Aachen, Germany

ABSTRACT: In the framework of the In-situ Stimulation and Circulation (ISC) experiment Fiber-Bragg-Grating (FBG) and Brillouin strain sensing systems were installed to monitor deformation during six hydraulic shearing and six hydraulic fracturing experiments. Three boreholes were dedicated to strain monitoring. Both systems are installed in the same boreholes, offering a unique opportunity to compare these systems with respect to their applicability in hydraulic stimulation tests. A total of 60 FBG sensors with 1 m base length were installed across fractures, shear zones and intact rock. Along the entire borehole length, pre-stressed optical cables for Brillouin distributed strain (DBS) sensing were embedded in grout with two installation methods: a bare cable and a cable packed and fixed with glue every 0.65 m. The strain signals were compared as time series for a given borehole depth and as profiles along the borehole axis. The study reveals that the FBG system gives a high accuracy (0.04 µ-strain) and temporal resolution (>1s) with pointwise measurements. The bare DBS leg yield good quantitative strain data with poorer strain accuracy (>500 times poorer than FBG) and poorer temporal resolution (factor of >100). The packed DBS leg provide no meaningful information about the strain field.

1. INTRODUCTION

Deformation is the fundamental kinematic variable in rock mechanics. Commonly, it is expressed as *strain*, which is the non-rotational component of the deformation tensor (i.e., the spatial derivative of the displacement field) (Jaeger et al. 2007). Strain or deformation measurements are important for a broad range of applications: from lab-scale test (e.g., compressional tests), over structural engineering (e.g., bridges; (Glisic et al. 2011)) to geotechnical engineering (e.g., mining, tunneling; (Valley et al. 2012)(Valley et al. 2012)) and to natural hazards (Moore et al. 2010). Conventionally, in-situ deformation measurements are executed using multi-point borehole extensiometers (MPBX) or inclinometers that present strong limitations in terms of sensitivity and spatial coverage(Madjdabadi et al. 2016). Fiber-optics-based strain monitoring systems are more and more used in geotechnical context, since they combine high resolution and long durability with insensitivity to electromagnetic noise and moisture (Madjdabadi et al. 2016).

In 1978, (Hill et al. 1978) introduced the Fiber-Bragg Grating (FBG) technology which uses backscattering of light at artificially induced damages (i.e., gratings) along optical fibers to monitor strain and temperature. Such a grating has a specific wavelength stop band. This stop band covers a specific wavelength which is completely backscattered (i.e., back-reflected) at this point. The rest of the wavelength spectrum is not affected by the grating and passes through. The basic principle of FBG sensing is the dependency of the specific wavelength stop band for each grating on variations in strain and temperature.

Along a single optical fiber typically more than 20 Fiber-Bragg Gratings (i.e., sensors) can be manufactured, as long as there is no overlap in their wavelength stop band (Iten 2011).

Since the late 1980s the distributed Brillouin sensing (DBS) technology has been used to monitor strain in optical fibers, including applications for monitoring of concrete and steel bridges, dams and embankments, and mining (Glisic et al. 2011; Valley et al. 2012; He et al. 2013). This technology uses the strain dependency of the acoustic wave velocity in the fiber core and measures the resulting frequency shift of the backscattered light. Two subtypes for this system can be distinguished: a) Brillouin Time Domain Reflectometry (BOTDR) and b) Brillouin Time Domain Analysis (BOTDA) (Madjdabadi et al. 2016). For this study we used a BOTDA system, which stimulates scattering by sending a constant light beam

from one end into the fiber and one light pulse into the other end.

As both fiber-optics based strain monitoring systems are based on different physics, they have different monitoring characteristics. In this study, we compare the two systems (i.e., FBG and DTS) qualitatively and quantitatively in terms of noise, the general response to deformation and captured strain magnitudes. In this paper we use the engineering mechanical convention, meaning that tensional stresses and strains are positive.

We conducted this study in the framework of the in-situ stimulation and circulation (ISC) experiment (Amann et al. 2018) at the Grimsel Test Site, Switzerland. During the ISC experiment six hydraulic shearing (HS) and six hydraulic fracturing (HF) test were conducted. For these tests, different shear zones, subdivided into two sets (i.e., referred to S1- and S3-orientation) (Fig. 1) have been hydraulically stimulated (i.e., during HS-tests) and in intact rock hydraulically fractured (i.e., during HF-tests). For both experiment types (HS and HF) we followed standardized injection protocols (Fig. 3a and 7a) that included various hydraulic loading cycles, including constant (i.e., pressure or flow-rate controlled) or oscillation loading (i.e., applied only during HF tests).

2. MONITORING LAYOUT

Three 44 to 47 m long boreholes (so-called FBS1, FBS2, and FBS3) were drilled into the rock mass to monitor the strain changes during the hydraulic stimulations (Fig. 1). FBS1 is oblique to both shear zone directions and penetrates through them. FBS2 is subparallel to the S3 shear zones, and FBS3 is subparallel to the S1 shear zones. Each borehole contains a total of 20 FBG sensors, distributed in two chains to ensure that one chain keeps measuring in case one chain is damaged. Each of the same boreholes contain two legs of the DBS cable installed in a loop configuration. Note that this loop configuration was required for our BOTDA (Brillouin Time Domain Analysis) system. Thus, one long DBS cable could be used, covering all three FBS boreholes. PVC injection pipes served as mounting system for the FBG sensors and the DBS cables. All three boreholes were completely equipped before grouting. Afterwards, the grout was injected through the injection pipe and thus the boreholes were filled from bottom to top to avoid any air inclusions. The mixture of the grout was chosen to replicate the elastic properties of the granitic host rock.

Prior to FBG sensor installation, the borehole was screened using an optical televiewer (OPTV) borehole probe. The sensors were placed into the borehole covering either host rock, fractures and/or shear zones (Fig. 1b). The FBG sensors used in this experiment are of the model os3600 by Micron Optics Inc. and have a base length of 100 cm. A strain accuracy of 0.85 µ-strain and a wavelength repeatability (i.e., resolution) of less than 0.1 µ-strain can be reached in combination with the used optical interrogator si255 by Micron Optics (latest generation of Hyperion Platform generators) at 1 Hz sampling rate. The maximum used sampling rate was 1000 Hz during the experiments.

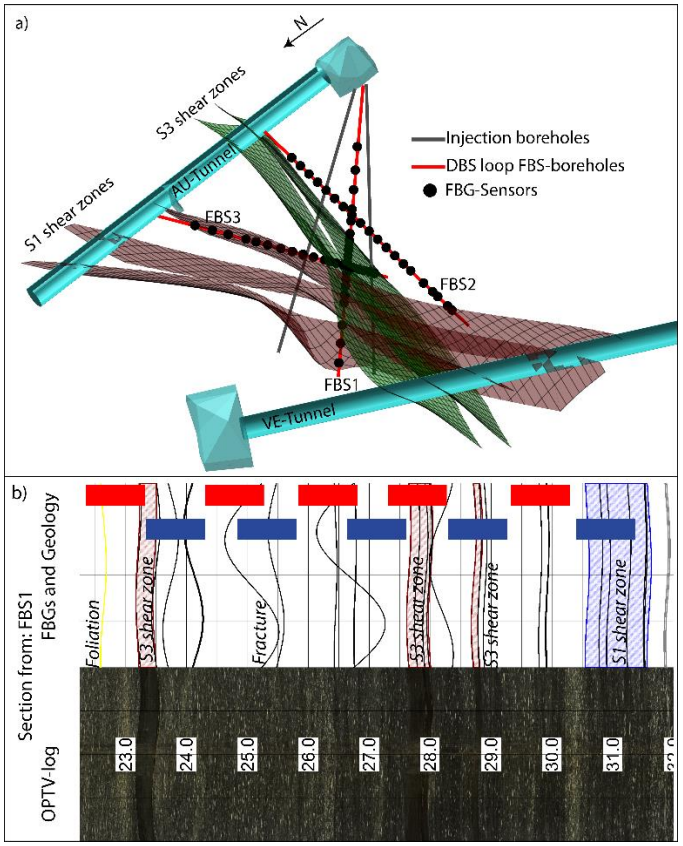

Fig 1. Illustration of sensor positions. A): The geological model of the test volume with indicated shear zones sets, Injection boreholes for stimulation, FBG-sensors and DBS fibers. B) Section of OPTV-log (with depth information in white boxes) from FBS1 with mapped geological structures and FBG sensors (red and blue boxes). Since the DBS fiber would be just a straight line, it was not plotted into this figure.

The DBS system was installed in two legs per borehole, due to the closed loop character of this system allowing two different mounting strategies. One leg was installed as a bare sensing cable along the injection pipe (fixed with zip ties), the other leg was mounted in a corrugated tube using glue points in regular intervals of 65 cm. This second installation procedure mitigates the insensitivity of the system to very localized strain. Indeed with this procedure very localized strain is distributed over 65 cm intervals which is assumed to be sufficient for this system (Madjdabadi et al. 2016). Both cables were slightly pre-strained (i.e., put under tension) to allow monitoring of tensional and compressional signals. The used sensing cable (BRUsens strain V1 single mode cable) has a diameter of 3.2 mm, and contains one single mode (SM) fiber suitable for Brillouin or Rayleigh scattering

technology. As optical interrogator a BOTDA unit (i.e., so-called DiTEST) by Omnisens was used. It achieves a strain resolution of 2 µ-strain and a spatial resolution of 0.5 – 1 m. The sampling rate depends on the frequency range that was covered by the probe beam, and varies between 4 and 8 minutes. Note that the actual sampling rate was lower (i.e., longer time intervals between measurements) in this test, since we connected two optical-fiber loops to the interrogator which can only measure one loop at a time. Due to a damage in the optical fiber we were able to measure the strain either in the FBS1 borehole, or in the FBS2 and FBS3 borehole at once. This additionally reduced the sampling rate during the DBS measurements.

3. NOISE LEVEL DETERMINATION

During a time span of roughly 36 h, during which no experiments (i.e., fluid injection tests) were conducted in the test volume, strains were measured with both systems to capture their noise level. This approach led to more than 2 million measurements for the FBG system, and 102 measurements for the DBS loop in FBS1 and 56 for the DBS loop in FBS2 and FBS3. The low number of data points for the DBS system is due to interruptions of the Omnisens Ditest software during the monitoring period, and the earlier mentioned low sampling rate.

As a first analysis step, the FBG strain data was corrected for linear temporal trends. Note that it was not cleared whether these linear trends are due to instrument shift of slow ongoing deformation that was not linked to the stimulation experiment. The linear trends were removed by fitting a linear function to the entire data and correct the data for the slope of this function. After removing the trends, the 10th and 90th percentile were calculated for each FBG sensor time series (Fig. 2a – upper panel).

Using this approach, outliers were removed, and the negative and positive range of noise was determined. The captured and corrected background strain signals varied between ±1µ-strain for all sensors along all three FBS boreholes. As a next processing step, 1000 strain recordings were averaged (i.e. down sampled to 1 Hz). To do so, we used a forward moving average. The percentiles were calculated for this reduced dataset, too (Fig. 2a – lower panel). After data reduction, the background strain signals varied between -0.04 µ-strain and 0.04 µ-strain along all three FBS boreholes.

For the DBS strain data averaging was not conducted due to the few data points. However, a spatial correction was conducted for the data, following the procedure published by (Madjdabadi et al. 2016). Along the optical cable the strain is measured at points with a constant spacing of 10 cm. Due to a spatial resolution of approx. 10 cm of the DBS system, each data point could have been measured at its real location, or within an interval of ± 10 cm. The correction compared true strain data with a reference measurement, and analyzed whether a certain data point fits best the true measurement point, or the one 10 cm before or after. This procedure removes spatial offsets between different time series and thus, filters positive and negative outliers from the noise signals. For detailed information about the correction method see (Madjdabadi et al. 2016). The 10th and 90th percentiles were calculated for the raw data and the spatially corrected data of each point along the optical fiber (Fig. 2b).

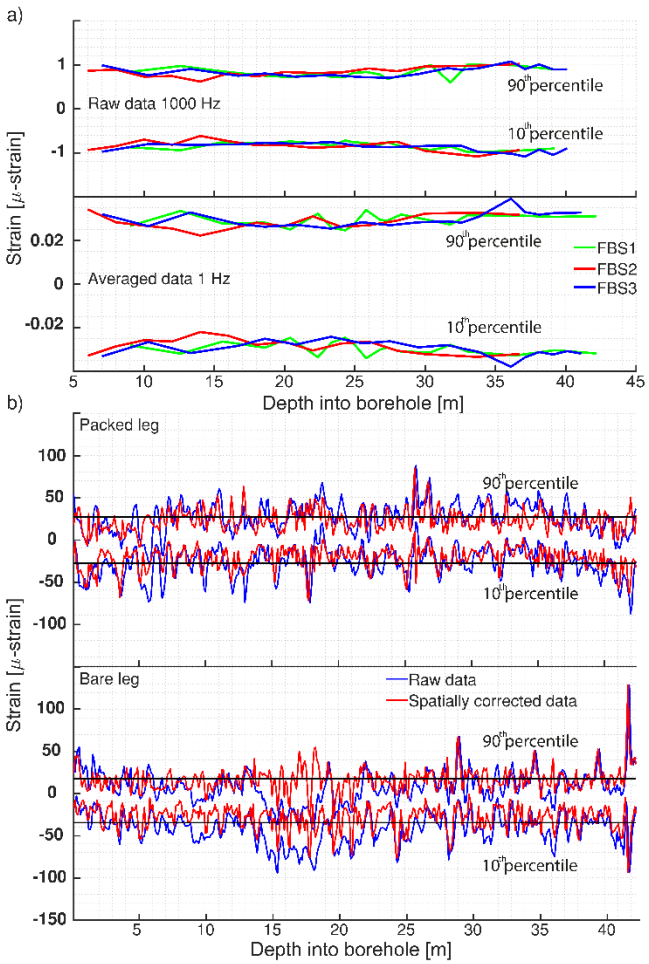

Fig 2. Visualization of background strain signals in µ-strain plotted against depth along boreholes. a) data from all FBS boreholes: upper panel: FBG raw data (1000 Hz); lower panel: averaged FBG data (1 Hz); b) DBS data from FBS3 showing raw (blue) and spatially corrected (red) strain values for bare leg (upper panel) and packed leg (lower panel), as well as the averaged noise level (black line) for both legs.

Afterwards, the calculated noise signals were averaged to calculate a unique background strain value for each borehole leg. For the raw dataset the background strain signals vary mostly between -30 and 45 µ-strain with some exceptions, where the strain signals range from -75 µ-strain to 85 µ-strain. The averaged background strains fall between -25 µ-strain and 25 µ-strain for the bare leg and between -30 µ-strain and 18 µ-strain for the packed leg. For further analysis, we used a background noise range from -30 µ-strain to 25 µ-strain. These noise levels

are comparable to those determined by (Madjdabadi et al. 2016).

4. OBSERVATIONS DURING A HYDROSHEARING (HS) TEST

The first monitoring performance analysis was done qualitatively using data captured with the FBG and DBS system in the borehole FBS1 during a HS experiment. The monitoring goals during the HS experiments were the high-resolution quantitative description of the deformation field (i.e., for FBG-sensors) and detection of splay fractures (i.e., for DBS system). During this analysis we examine trends in strain signals along borehole axis and over time. For the FBG system only the data averaged over 1000 samples were used for further analysis. The two different DBS legs (i.e., bare and packed leg) were treated as different systems here. In contrast to the noise determination, the DBS data were not spatially corrected during this analysis, since the applied strain rates were too high at well-localized measurement points for this procedure. Applying the aforementioned correction method might have led to an incorrect shift in strain signals, since the correction method depends on strain peaks in the background noise. If a measurement point at location x measured a true, large positive strain signal and the background noise was negative at this same location, but positive at the location x+1, the true strain peak was shifted to x+1, which may introduce erroneous results.

To visualize the trend in strain data along borehole axis, we defined a fixed time (i.e., 13:51 h on 9 Feb 2017) during which strain signals were analyzed. For both legs of the DBS system every measurement point along the borehole axis was considered as an individual data point.

To analyze the trends in strain signals over time we defined a fixed depth interval between 26.8 m and 27.8 m in FBS1. This interval is entirely covered by one FBG sensor. Nine DBS measurement points were located within this interval for both legs. For this analysis step we averaged the DBS measurement points of the bare leg within this interval. Thus, they covered the same interval as the FBG base length. For the packed leg, we averaged the strain signals that were recorded between two glue points within the test interval (i.e., between glue points at 27.0 m and 27.65 m depth). Afterward, each DBS obtained time series was smoothed using a moving average over two neighboring data points. Note that the strain signals presented here are related to the hydraulic stimulation, which followed the fluid injection protocol shown in Fig. 3a and was similarly applied also for the other experiments (Amann et al., 2018). During each stimulation experiment, the rock volume was pressurized in four cycles, with the highest injection volume in cycle three.

4.1 FBG-system

The time series analysis of the depth interval between 26.8 m and 27.8 m revealed four tensional peaks in the strain signal (Fig. 3b). Those peaks were due to the above-mentioned stimulation loading cycles. From 10:24 h on the strain signals were permanently tensional, with the peaks at 11:01 h, 12:14 h, 13:50 h, and 15:51 h. Note that the FBG data indicate a permanent strain signal after the last stimulation cycle, which can be interpreted from the asymptotic behavior of the FBG sensor towards 35 µ-strain.

The time series for the depth interval between 42.2 m and 43.2 m shows constantly compressive strain signals from 10:24 h on. Four compressional peaks are obtained with magnitudes ranging between -5 µ-strain and -43 µ-strain. These compressional signals occur at the same time as the tensional ones at 26.8 m depth. Note that the time series contain a permanent compressional strain signal of -22 µ-strain.

For the reference time t shown in Fig. 3b, all FBG sensors recorded strain signals larger than the above-determined noise level. Negative (i.e., compressional) strain signals are obtained between 10 m and 20 m, and below 33 m along the borehole axis. Positive strains (i.e., tensional) are observed between 20 m and 33 m depth (Fig. 3c). Within this interval, our data indicates two strain peaks: one smaller one between 22.33 m and 23.33 m depth and one with a larger magnitude between 26.8 m and 27.8 m.

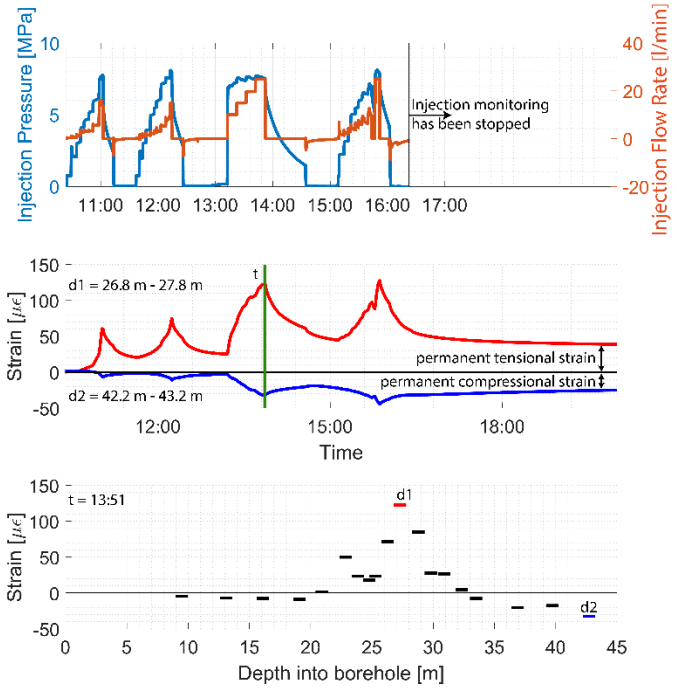

Fig 3. Visualization of the fluid injection protocol (upper panel) with four separate injection cycles. The middle panel shows the time series for the FBG sensors at 26.8 m and 42.2 m depth. The reference time chosen for the depth profile is indicated as vertical line (in green). In the lower panel the depth profile is

shown which was recorded at 13:51. The sensors used for the time series analysis are color-coded.

It is assumed that mode I fracture opening creates high magnitude strain signals, which are mostly reversible, whereas mode II or III dislocation along fracture have a strong irreversible strain component. Thus, the combination of reversible and irreversible strain signals is captured at 26.8 m, indicating two deformational components: normal fracture opening (i.e., mode I) and shear dislocation (i.e., mode II or III). Thus, the strain signal from 26.8 m is interpreted to represent a permanent strain component that is associated with the maximum reached shear dislocation, whereas the difference in magnitude between peak strain and permanent strain provides a measure of the maximum normal fracture opening.

The compressional signals at 42.2 m are interpreted as a combination of 1) a poroelastic effect, producing compression in the far-field of injection as the rock mass gives way to the injected volume, and 2) an irreversible, compressional deformation in the near field of the stimulation zone.

4.2 DBS-system bare leg

The time series, obtained by the bare DBS leg between 26.8 m and 27.8 m, indicates, with few exceptions, tensional strains from 10:24 h on (Fig. 4a). During this tensional strain series, three peaks are observed at 12:12 h, 13:58 h, and 15:46 h. Including the minor peak at 11:03 h, the bare DBS leg captures the same four tensional peaks over time, as the FBG system. Note, that the bare DBS leg indicates a permanent strain signal after the last peak, in agreement with the FBG system. The final strains vary around 50 µ-strain.

The time series averaged for the depth interval between 42.2 m and 43.3 m shows constantly compressional strains. From the data, no peaks in compressional signal are obtained. However, the data indicates a permanent compressional strain signal of <26 µ-strain.

For the upper most 12.5 m along the borehole axis, the bare-leg DBS data show strain signals below the noise level (Fig. 4c). Between 12.5 m and 13.5 m the fiber measures a small tensional signal, followed by a compressional signal between 16 m and 20.5 m. Note that these two signals are not observed in the FBG system. However, the two tensional peaks between 22.5 m and 23.2 m (peak at 22.9 m), and 25.9 m and 28.79 m (peak at 27.7 m) fit the FBG signals well. Between 33.59 m and 35.6 m into the borehole, the bare leg records an additional strong tensional peak. Note, that it is known from the conducted OPTV-log, that FBS1 is intersected by fractures at 33.61 m and 35.83 m depth. Thus, it seems likely that the bare DBS leg captured true deformations at these locations. These peaks are recorded neither in the FBG system, nor in the packed DBS leg. Below 36.1 m borehole depth, the bare leg records continuously compressional strains, in agreement with the FBG signals.

The bare DBS leg indicates strain data along the borehole axis and over time, that fit the FBG obtained data well, as soon as the strain magnitude exceeds the noise levels. The overall trends in strain signals are consistent for both tension and compression.

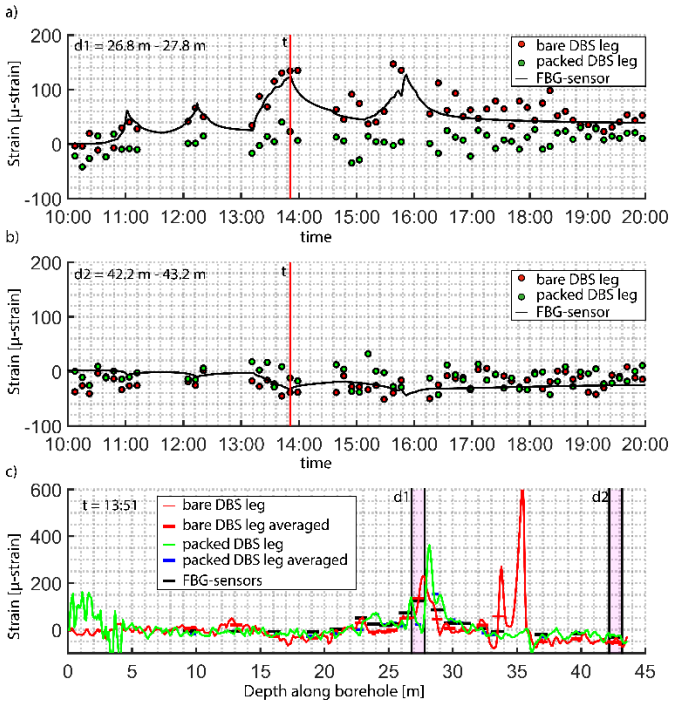

Fig 4. Visualization of the DBS data. a) and b) show the time series for the same depths as analyzed for FBG sensors with a separation for the bare and packed leg. c) shows the depth profile at the same reference time as chosen for the FBG analysis. Within the diagram, the raw DBS data and the averaged data at FBG locations are indicated.

4.3 DBS system packed leg

For the packed leg, the strains signals were not averaged between 26.8 m and 27.8 m, and 42.2 m and 43.2 m, but between the glue point interval within this depth intervals (Fig. 4a & b). The packed leg measures strain signals at 26.8 m depth within the noise level until 13:34 h. Between 13:42 h and 14:38 h tensional signals are recorded with a peak at 13:50 h. This peak aligns well with the data from the FBG system and the bare DBS leg. After this real tensional period, the data continued indicating mostly tensional signals, that were mostly within the noise level.

The time series for the glue point interval between 42.2 m and 43.2 m obtains strain data that are mostly compressional. These data loosely follow the trends that are already seen in the bare DBS leg. However, the magnitudes in the packed DBS leg are smaller (Fig. 4b)

and this time series do not indicate a permanent compressional strain signal.

The packed DBS leg measures tensional strain signals in the top 5 m of the borehole. These signals are due to a known damage in the optical fiber and are not further considered. Between 5 m and 18.79 m depth, the packed leg strains are within the noise range (see Fig. 4), followed by few compressional signals above 20.9 m. Deeper along the borehole axis, two tensional peaks are observed between 22.9 m and 24.4 m (peak at 24 m), and 26.0 m and 30.6 m (peak at 27.9 m). Note that these peaks are recorded slightly deeper (i.e., 0.5 m – 1 m) in the borehole than the corresponding peaks in the bare leg. From 33.5 m on, the packed leg data shows strain signals that are mostly within the noise level, with some compressional components.

4.4 Comparison

FBG and bare DBS leg measurements show consistent trends in strain values, while the packed DBS leg data is of poorer quality. Compared to the FBG system and bare DBS leg the packed DBS leg measures smaller strain magnitudes. This was in part expected because localized strain gets distributed over a longer cable section, however this should also be the case for the FBG sensors with 1 m base length. Also, a downhole shift of the packed DBS leg data is observed with respect to the FBG system and bare DBS leg. This shift could be due to the averaging of 0.65 cm for the packed DBS leg, whereas the other two systems show signals that are averaged over 1 m. Even though the overall trend in the strain signal might be similar for both DBS legs, it is not very reliable in the packed leg, due to the small signal/noise ratio. In contrast, the bare DBS leg and the FBG sensors give comparable strain within the noise level of the DBS system.

A quantitative comparison between strain magnitudes is visualized in Fig. 5. This comparison is conducted for the same reference depths and time as used before. The monitoring data indicates that for the two depth intervals the bare DBS leg shows stronger signals than the FBG sensor, whereas the packed DBS leg signals are weaker. The packed DBS leg even obtains compressional strains, while bare DBS leg and FBGs measures tensional strains. The large deviation from the FBG signals might be explained by the high background noise of the DBS legs. Note that for higher FBG-obtained strain signals (>90 µ-strain) this deviation reduces to almost 10 µ-strain for the packed leg. Nevertheless, the packed DBS leg constantly shows weaker signals than the FBG signals. The only exception is the point where the FBGs obtained almost no strain (i.e., ± 5 µ-strain). At this point the DBS legs measures pure background noise.

For the fixed reference time (Fig. 5b) the profile along the borehole indicates mismatches between FBG and DBS system of larger than ±10 µ-strain. Both DBS systems mostly underestimate the FBG signals, with some exceptions. Over the entire range of FBG obtained strain signals, some DBS signals with deviations of less than 90 µ-strain are observed.

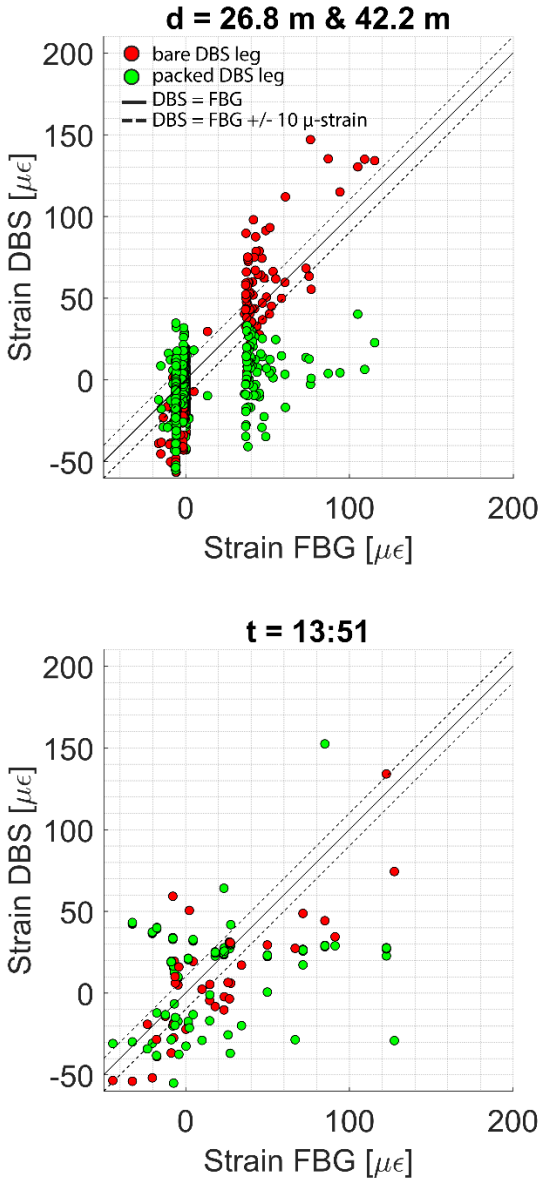

Fig 5. Quantitative comparison of FBG and DBS sensors. a) shows FBG and DBS time series comparison summarizing two depth intervals. b) visualizes the correlation between FBG and DBS during a defined reference time.

5. OBSERVATIONS DURING A HYDRAULIC FRACTURING (HF) TEST

To compare the spatial resolution of the FBG and DBS system we analyzed data from a hydraulic fracturing test that were recorded in the FBS2 hole. During these tests, the monitoring aimed for a quantification of the deformation field, with a special interest in tracing of hydraulic fractures to determine their propagation directions. The data of both systems were processed as

described in Section 4. For the analysis of the spatial resolution we chose 14:10 h 16 as reference time (Fig. 6a). The FBG sensors indicate a tensional strain signal between 20.0 m and 21.0m with a magnitude of 700 µ-strain. Below and above this interval the FBG sensors observe compressional strain signals with a magnitude ranging from -36 µ-strain to -80 µ-strain (Fig. 6b). A permanent strain signal (50 µ-strain) is measured for the FBG sensor at 20.0 m (Fig. 6a). Thus, it is assumed that the well localized high tensional strain signal is due to the normal opening (mode 1) of a distinct fracture, which might have been reactivated or initiated as a hydraulic fracture. This permanent strain signal is comparably small with respect to the reversible part of the strain signal, but in the same order of magnitude with respect to the permanent strain signal obtained during the presented HS test.

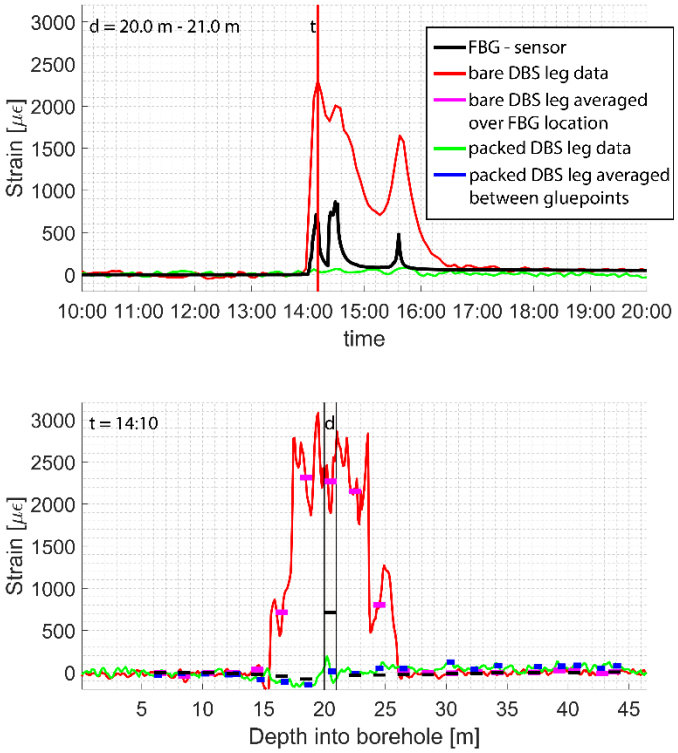

Fig 6. Strain data measured during hydraulic fracturing experiment. a) shows time series and b) the profile along the borehole axis.

Along the bare DBS leg, tensional strain signals are measured between 16.0 m to 26.0 m along the borehole axis with a peak magnitude of 3078 µ-strain. Averaging the strain data over FBG base lengths reduces the tensional strain magnitude to 2268 µ-strain, which is still > 3times larger than the FBG obtained magnitude at the 20.0 m. Note, that these strain signals might be explained by opening of several fractures which are located between the FBG sensors. However, this would require to also show compressional strains for the averaged the bare DBS leg signals at the FBG locations. The fact, that the averaged bare DBS data are missing compressional signals at these locations, might indicate slight debonding of the bare fiber. Note that the tensional signal of the DBS leg drops at the locations of the FBG sensors. A potential drop in pre-strain of the bare DBS leg, due to a construction problem, might explain the lag of true compressional signals between the distinct tensional peaks at the FBG locations in this theory.

The packed DBS leg reveals a tensional strain peak at 20.21 m depth with a magnitude of 190 µ-strain. Above and below this depth the data shows compressional strain signals, varying between -122 µ-strain and -150 µ-strain. Thus, the spatial trend in the packed DBS leg data is similar to the FBG signal, indicating one single tensional strain peak between 20.0 m and 21.0 m. However, the DBS magnitude is smaller than the FBG obtained magnitude by a factor of 3.

As the following processing step, the packed DBS leg signals were averaged for the glue point intervals which mostly cover the FBG base lengths. The resulting data indicates higher compressional strain above (i.e., < 20 m depth) the tensional peak, compared to the FBG sensors. Below this peak, this relationship is reversed. Note that the actual tensional peak is located at 20.21 m depth, whereas the glue point interval started at 20.3 m. This indicates that the strain signal measured by the FBG sensors might be heterogeneous over the sensor base length. Thus, it is useful to average the packed DBS data not just for the glue point interval that covers most of the FBG base length, but for all intervals that cover the FBG base length.

6. CONCLUSIONS

The study highlights the differences in the applicability of different fiber-optics systems. It was demonstrated that the FBG system provides a high-resolution quantitative measure of the spatial deformation field that was assumed to represent ground truth information. The sensors proved a high accuracy in strain magnitude and temporal resolution. Besides these advantages, however, the FBG sensor has a pointwise measurement characteristic, due to a fixed base length.

The bare DBS leg obtained time series of strain signals that follow the trends measured by the FBG sensors. However, in terms of magnitude, the bare DBS leg signals seem to provide only a qualitative measure, due to the high deviations from the FBG magnitudes. Along the borehole profile, the bare DBS leg follows the trends of the FBG system well. The major advantage of the bare DBS leg is that it obtains strain data distributed along the entire borehole axis, even though they are just qualitative measures. As shown in the HF test, the optical cable was very sensitive to the installation problems. Even though this system was not perfectly suitable for the stimulation experiment (i.e., due to slow sampling rate and qualitative

magnitude measures), it might be useful in engineering contexts, where slow strain changes and larger strain magnitudes occur.

In contrast to the bare DBS leg, obtained the packed DBS leg strain signals that did not well follow the FBG data temporally and spatially. The packed legs were not sensitive enough to capture the strain signals, even though they exceeded the background noise level. This insensitivity might be explained by insufficient fixing at the glue points. Thus, the fiber was not divided into static intervals, but likely was divided by glue points at which slight debonding occurred. Therefore, the cable was allowed to slightly move at these points, making the fiber less sensitive for strain signals. In contrast to Madjdabadi et al., (2016), we were not able to gain well localized strains.

Based on our results, we suggest to use FBG technology for projects, where the areas (e.g., locations along boreholes) of interest are known and high strain accuracy and temporal resolution are desired. For projects with uncertain or larger areas of interest and larger expected strains, we suggest DBS with bare-leg installation, while packed leg DBS – at least in our experiment – did not yield reliable data.

Acknowledgements

The ISC is a project of the Deep Underground Laboratory at ETH Zurich, established by the Swiss Competence Center for Energy Research - Supply of Electricity (SCCER-SoE) with the support of the Swiss Commission for Technology and Innovation (CTI). Funding for the ISC project was provided by the ETH Foundation with grants from Shell and EWZ and by the Swiss Federal Office of Energy through a P&D grant. Hannes Krietsch is supported by SNF grant 200021_169178. We like to thank Marmota for the successful installation of the optical fibers for the DBS system and the FBG sensors. The Grimsel Test Site is operated by Nagra, the National Cooperative for the Disposal of Radioactive Waste. We are indebted to Nagra for hosting the ISC experiment in their GTS facility and to the Nagra technical staff for onsite support.

References

1. Amann F, Gischig V, Evans KF, et al (2018) The seismo-hydro-mechanical behaviour during deep geothermal reservoir stimulations: open questions tackled in a decameter-scale in-situ stimulation experiment. Solid Earth Discussions. doi: 10.5194/se-2017-79

2. Glisic B, Chen J, Hubbell D (2011) Streicker Bridge: a comparison between Bragg-grating long-gauge strain and temperature sensors and Brillouin scattering-based distributed strain and temperature sensors. International Society for Optics and Photonics, p 79812C

3. He J, Zhou Z, Jinping O (2013) Optic fiber sensor-based smart bridge cable with functionality of self-sensing. Mech Syst Signal Process 35:84–94. doi: 10.1016/j.ymssp.2012.08.022

4. Hill KO, Fujii Y, Johnson DC, Kawasaki BS (1978) Photosensitivity in optical fiber waveguides: Application to reflection filter fabrication. Appl Phys Lett 32:647–649. doi: 10.1063/1.89881

5. Iten M (2011) Novel Applications of the Distributed Fiber-Optic Sensing in Geotechnical Engineering. Doctor of Science, ETH Zurich

6. Jaeger JC, Cook NGW, Zimmerman RW (2007) Fundamentals of Rock Mechanics, fourth. Blackwell Publishing Ltd

7. Madjdabadi B, Valley B, Dusseault M, Kaiser PK (2016) Experimental evaluation of a distributed Brillouin sensing system for measuring extensional and shear deformation in rock. Measurement 77:54–66. doi: 10.1016/j.measurement.2015.08.040

8. Moore JR, Gischig V, Button E, Loew S (2010) Rockslide deformation monitoring with fiber optic strain sensors. Nat Hazards Earth Syst Sci Katlenburg-Lindau 10:

9. Valley B, Madjdabadi BM, Kaiser PK, Dusseault MB (2012) Monitoring Mining-induced Rock Mass Deformation Using Distributed Strain Monitoring Based On Fiber Optics. International Society for Rock Mechanics and Rock Engineering